A biosensor of Src family kinase conformation by exposable tetracysteine useful for cell-based screening.

Sevgi Irtegun[1,2], Rebecca Wood[1,2],Kurt Lackovic[3,4], Jörg Schweiggert[1], Yasmin M. Ramdzan[1], David C.S. Huang[3,4], Terrence D. Mulhern[1*] & Danny M. Hatters[1*]

[1]Department of Biochemistry and Molecular Biology; and Bio21 Molecular Science and Biotechnology Institute, University of Melbourne, VIC 3010.

[2]Equally contributed to the work.

[3]Walter and Eliza Hall Institute of Medical Research, VIC 3010

[4]Department of Medical Biology, University of Melbourne, VIC 3010

*Correspondence should be addressed to D.M.H. (dhatters@unimelb.edu.au) or T.D.M. (tmulhern@unimelb.edu.au) . Ph: +61 38344 2530.

ABSTRACT

We developed a new approach to distinguish distinct protein conformations in live cells. The method, exposable tetracysteine (XTC), involved placing an engineered tetracysteine motif into a target protein that has conditional access to biarsenical dye binding by conformational state. XTC was used to distinguish open and closed regulatory conformations of Src family kinases. Substituting just four residues with cysteines in the conserved SH2 domain of three Src-family kinases (c-Src, Lck, Lyn) enabled open and closed conformations to be monitored based on binding differences to biarsenical dyes FlAsH or ReAsH. Fusion of the kinases with a fluorescent protein tracked the kinase presence, and the XTC approach enabled simultaneous assessment of regulatory state. The c-Src XTC biosensor was applied in a boutique screen of kinase inhibitors, which revealed six compounds to induce conformational closure. The XTC approach demonstrates new potential for assays targeting conformational changes in key proteins in disease and biology.

Our knowledge of the mechanical operation of proteins in live cells has remained difficult to determine due to a dearth of methods. Fluorescence resonance energy transfer (FRET) has been a major method, particularly in the development of metabolite biosensors (*1*), but is not suitable for all systems and contexts. For assessing conformational changes in proteins, FRET typically requires the expression of two fluorescent protein fusions to a target protein, which may be difficult to accommodate without major impedance to protein function. The emergence of chemical biology avenues offers much potential to greatly expand the repertoire of methods to address these challenges. One example is the capacity of a tetracysteine

(TC) motif, CCXXCC, to bind biarsenical fluorophores FlAsH and ReAsH with high affinity and specificity in live cells (*2*). The binary nature of the system and small size of the dyes have enabled innovative applications for investigating protein self-association, folding and oligomerization (*3-5*).

Here, we describe a new approach for tracking alternate conformations of Src family kinases (SFKs) using an exposable tetracysteine (XTC) sequence with conformation-specific biarsenical dye reactivity. SFKs modulate signaling pathways that drive cell growth, differentiation, proliferation, apoptosis, adhesion and migration. They are overactive in a wide variety of human cancers, making them attractive therapeutic targets (*6*). SFKs have "open" active and "closed" inactive conformations that are well understood at an atomic level (*7, 8*) (Fig 1a). The activity of c-Src in terms of the local balance of the upstream kinase and upstream phosphatase activities can now be measured spatially in live cells using FRET reporters of the phosphorylation status of a c-Src substrate (*9*); however, its regulatory state remains more challenging to monitor. Prior work established an approach involving microinjection of an extrinsic probe that selectively binds the SFK SH3 domain in the open conformation (*10*). This method is highly sensitive, but not amenable for high throughput assays and does not discriminate between different SFK members (*11*).

By introducing mutations R159C, E160C, R163C and L164C in the SH2 domain of human c-Src, we created an exposable TC construct (c-Src^{XTC}) predicted to be solvent exposed only in the open state and have a geometry permissive to FlAsH and ReAsH binding (*7, 8, 12*) (Fig 1a). To test whether c-Src^{XTC} bound biarsenical dyes in a conformation-specific manner, the construct was superimposed onto "open" active or "closed" inactive mutant backgrounds and transiently expressed in AD293 cells under a high yielding CMV promoter. c-Src$^{XTC}{}_{open}$ and c-Src$^{XTC}{}_{closed}$ have additional

mutations (Open: Y530F and closed: Q531E, P532E, G533I) that alter the affinity of the C-tail to the SH2 domain, an interaction which stabilizes the closed form (*13*). To provide an independent measure of c-Src expression and localization, the monomeric GFP variant Emerald was fused to the C-terminus, via a linker sequence previously validated to preserve the major functionality of c-Src (*14*) (Fig 1b).

c-Src^{XTC}, c-Src$^{XTC}_{open}$ and c-Src$^{XTC}_{closed}$ were assessed for ReAsH red-fluorescent biarsenical dye reactivity in live cells, relative to a negative control (c-Src^{NTC}) with no TC tag, and a positive control (c-Src^{CTC}) that had the TC tag appended in a highly accessible position on the C-terminal of Emerald (Fig 1b, Supplementary Table 1). c-Src$^{XTC}_{open}$ had approximately 80% of the fluorescent yield of the positive control, c-Src$^{XTC}_{closed}$ was similar to the negative control and c-Src^{XTC} was intermediate between open and closed variants (Fig 1c). These data indicate that c-Src^{XTC} reports on c-Src conformation with good differential in the signal between the open and closed states.

For a more quantitative and high throughput assessment using flow cytometry, we adapted the reporter color scheme for standard flow cytometry filter sets and laser combinations (to which ReAsH is not well-suited). The Emerald moiety was replaced with the monomeric Cerulean fluorescent protein and the binding of the TC tag was examined with the green-fluorescent biarsenical dye FlAsH. Cytograms plotting Pacific-Blue (for Cerulean) versus FITC (for FlAsH) confirmed conformation-dependent differences in FlAsH reactivity, similar to the patterns observed by microscopy with the Emerald/ReAsH combination (Fig 2a). A simple quantitative measure of "closure" was found by gating for high FlAsH fluorescence and calculating the percent of cells within this gate (Fig 2a, 2b). The majority of cells expressing c-Src$^{XTC}_{open}$ were high-FlAsH-reactive, whereas the majority of those expressing c-Src$^{XTC}_{closed}$ were low-FlAsH-reactive (Fig 2a, 2b).

To make the reporter more generally useful as a tool for the study of SFKs, we examined whether other members of the family could be converted into biosensors of open and closed conformations using the same strategy. The exposable TC motif was introduced at the equivalent SH2 locations of Lyn and Lck and the biosensors were superimposed onto open and closed mutant backgrounds. The Lck and Lyn sensors also exhibited conformation-sensitive FlAsH reactivities (Fig 2b). All c-Src^{XTC}, Lck^{XTC} and Lyn^{XTC} had FlAsH reactivities significantly higher than those of their respective closed variants (Fig 2b). Because SFKs are largely inactive under basal conditions (*15*), our results raise the possibility that XTC mutations shift the conformational equilibrium towards the open state. Examination of the ability of the SFKs to phosphorylate substrate STAT3 found that the XTC mutations led to an increased basal kinase activity (Fig 3a). The SH2 domain of c-Src^{XTC} remained folded (Fig 3b) but had a three-fold decreased binding affinity to phosphotyrosine (Fig 3c), which accounts for the destabilization of the closed state. In addition, we cannot exclude the possibility that the mutated residues abrogate direct or water-mediated electrostatic interactions with the C-lobe of the kinase domain of Src. This may limit the application of the biosensors to physiological problems. However, the shift towards the open state provides the dynamic range required to enable screening for compounds that induce closure.

Therefore, we next assessed whether the XTC sensors can be used to assay drugs for their effect on c-Src conformation. To our knowledge, there are no high-throughput drug screening platforms that assess changes in the regulatory state of SFKs in live cells, which have the potential to be used to identify inhibitors with novel mechanisms of action. To test for this capability, the c-Src^{XTC} biosensor was screened against a library of 72 kinase inhibitors that had no inherent fluorescence based on a

pre-screen on untransfected cells. After a 2 hour treatment with the drugs at 5 μM, COS-1 cells were labeled with FlAsH and analyzed by flow cytometry. The screen identified drugs that appeared to induce c-Src closure as well as those that appeared to open c-Src; however, the majority had no statistically significant effect on c-Src^{XTC} conformation, including compounds known to inhibit c-Src (Supplementary Table 2). This is unsurprising since the majority of kinase inhibitors target the ATP binding site in the active DFG-in conformation (as opposed to the catalytically inactive DFG-out conformation) (*16*), and would therefore not be expected to induce c-Src closure. For example, the clinical c-Src and BCR-Abl inhibitor bosutinib binds c-Src in the DFG-in conformation (*17*) and produced no significant change in FlAsH binding in the drug screen (p=0.64; Supplementary Table 2). By assaying conformation rather than activity, the biosensor has the potential to identify inhibitors with novel mechanisms of action, and potentially how changes in the cellular signaling landscape impact on Src conformation through indirect pathways. Six compounds that increased c-Src closure were identified: PP1, PP2, tozasertib, CYC116, vandetanib and N2-[4-(Aminomethyl)phenyl]-5-fluoro-N4- phenylpyrimidine-2,4-diamine. Vandetanib targets EGFR and VEGFR (*18*); however, it has been shown to bind and inhibit c-Src (*19*). Tozasertib and CYC-116 target Aurora kinases (*20*, *21*) and are reported to inhibit c-Src (*22*). N2-[4-(Aminomethyl)phenyl]-5-fluoro-N4-phenylpyrimidine-2,4-diamine is a pan kinase inhibitor; however, to our knowledge there is no available data specific to c-Src. PP1 and PP2 are gold standard c-Src inhibitors, with IC_{50} values of 50 nM and 100 nM, respectively in *in vitro* kinase assays (*23*).

We further validated PP1 and PP2 by concentration-response curves to calculate the half maximal effective concentration (EC_{50}) for c-Src^{XTC} conformational shift (Fig 4). Both PP1 and PP2 EC_{50} values were estimated to be in the low micromolar range.

These values agree with other cell-based dose response data for PP2 (*24*); however, they are over two orders of magnitude greater than the *in vitro* IC_{50} values. These results demonstrate limitations of *in vitro* data for biological problems and highlight the importance of cell-based assays in drug development.

Notably, no drugs induced complete closure of c-Src^{XTC}. Both PP1 and PP2 reduced percent of high FlAsH cells from over 80% to just under 70% (Fig 4), whereas the closed mutant had approximately 30% high FlAsH (Fig 2b). The drugs are likely to alter the equilibrium between open and closed conformations; how this occurs remains to be determined. One possibility is that drug-induced changes in the active site conformation further toggle the open and closed states. Another consideration is that the high expression level of the SFKs in our assays may lead to hyperphosphorylation of the activation loop, which conceivably influences the potency of the drugs for conformational change.

In summary, we have developed a novel genetically encoded biosensor to study conformation of three SFKs: c-Src, Lck and Lyn with just 4 point mutations. Thus the XTC biosensor strategy provides a new capability to study modulation of SFK conformation in living cells and is in principle adaptable to other proteins, especially those to which detailed structural knowledge is available for modeling.

FIGURE LEGENDS

Figure 1. Designing tetracysteine exposure to indicate c-Src conformation. a) The location of cysteine mutations in the SH2 domain of the c-Src^{XTC} sensor are modeled on the crystal structures of open (1Y57) and closed (2SRC) c-Src with ReAsH predicted to selectively bind the open conformation. **b)** Three basic variants

were used in this study. c-Src^{XTC} (exposable TC) binds biarsenical dyes (FlAsH or ReAsH) only in the open conformation. c-Src^{CTC} (constitutive TC) binds biarsenical dyes regardless of conformation due to a tetracysteine tag at the C-terminus of the fluorescent protein fusion. c-Src^{NTC} (no TC) lacks a tetracysteine tag. **c)** Confocal micrographs of AD293 cells expressing c-Src^{XTC} superimposed onto open or closed mutant backgrounds. All variants are fused to Emerald fluorescent protein.

Figure 2. The exposable TC sensor is adaptable to multiple SFKs a) Gating strategy for flow cytometry analysis showing FlAsH-labeled AD293 cells expressing Cerulean-fused c-Src$^{XTC}_{open}$ (blue) or c-Src$^{XTC}_{closed}$ (red). Cells were gated first for high expression then for high or low FlAsH. The percent of high expressers that are high FlAsH reactive was used for sample analysis. **b)** c-Src^{XTC}, Lck^{XTC} and Lyn^{XTC} biosensors successfully distinguish open and closed mutant backgrounds using flow cytometry. Shown are means ± S.E., n=3. **, $p<0.01$; ***, $p<0.001$; one tailed t-test.

Figure 3. Effect of exposable TC mutations on structure and activity of SFKs. a) Kinase activity of SFKs as indicated by levels of phosphorylated substrate STAT3 (pSTAT3), compared to total STAT3. **b**) Circular dichroism spectra of the purified no TC (NTC) and TC-containing (XTC) SH2 domains indicate the tetracysteine-containing domain folds properly. **c)** Binding curves for the interaction of the SH2 domains with the high affinity pYEEI peptide ligand. The fluorescence anisotropy of FITC-labeled peptide was measured versus protein concentration. Error bars on data points indicate S.E. from 5 repeated-measures. The TC mutation caused a decrease in affinity of the SH2 for the peptide (K_d from 0.43 ± 0.07 μM to 1.50 ± 0.21 μM; errors indicate S.E. of the estimate from the fit).

Figure 4. c-Src^{XTC} detects inhibitor-induced conformational closure.

Concentration response curves are shown for two hits from the drug screen, SFK

inhibitors PP1 and PP2. Error bars show means ± S.E. (n=8), reported error in EC_{50} values are S.E. of the estimate from the fit.

METHODS

DNA constructs. c-Src (NP_005408), Lyn (NP_002341) and Lck (NP_005347) cDNA appended C-terminally with linkers encoding amino acids GSGSDPPVAT, GSGSGSDPPVAT, AGSGSGSDPPVAT respectively, as well as XTC variants thereof (R159C, E160C, R163C, L164C), (K137C, D138C, R141C, Q142C) and (K135C, D136C, R139C, Q140C) respectively, were commercially synthesized using human-optimized codons and cloned into pT-Rex (Life Technologies). Cerulean, Emerald (*25*) and the C-terminal amino acid sequence CCPGCC (for c-$Src^{CTC)}$ were introduced via PCR-mediated cloning. Open (Src: Y530F; Lyn: Y508F; Lck: Y505F) and closed (Src: Q531E, P532E, G533I; Lyn: Q509E, Q510E, Q511I; Lck: Q506E, P507E, Q508I) mutations were introduced using QuikChange mutagenesis (Strategene).

Cloning & expression of the SH2 domain. SH2 sequences (residues 145–249) were cloned via PCR from c-Src^{XTC} and c-Src^{NTC} into pET21(d). A 6×His-tag was added to the N-terminus of the $SH2^{XTC}$ by PCR-mediated cloning. Proteins were expressed in BL21(DE3) *E. coli* and purified by phosphotyrosine affinity chromatography ($SH2^{NTC}$) or Ni^{2+}-affinity chromatography ($SH2^{XTC}$) to >95% purity. Correct masses were confirmed using a 6510 Q-TOF LC/MS (Agilent Technologies).

Mammalian cell culture. AD293 and COS-1 cells were maintained in DMEM supplemented with 10% FCS, 1 mM glutamine, 100 U/mL penicillin and 100 U/mL streptomycin in a humidified incubator with 5% CO_2.

ReAsH staining and imaging. 8×10^4 AD293 cells were plated into 8-well μ-slides (Ibidi) pre-coated with 0.01% (w/v) poly-L-lysine and transfected the following day with 0.5 μg of DNA using Lipofectamine 2000. After 24 hours, cells were labelled for 30 min with 10 μM 1,2-ethanedithiol (EDT), 2.5 μM ReAsH (Life Technologies) in HBSS then washed for 15 min in 250 μM 2,3-dimercaptopropanol (BAL) in HBSS. Cells were fixed with 3.2% (w/v) paraformaldehyde for 15 min at room temperature then imaged by a TCS SP2 confocal microscope (Leica). Emerald and ReAsH fluorescence were collected using 458 nm and 543 nm excitation lasers and emission wavelengths of 510–530 nm and 580–640 nm, respectively.

Western Blotting. Western blotting was performed as described previously (*13*). Blots were matched for total STAT3 then equivalent blots were probed for phospho-STAT3 or GFP (for SFK levels). Antibodies used were 1:10,000 anti-GFP from Life Technologies, 1:1,000 anti-STAT3 from BD Biosciences and 1:1,000 anti-phospho STAT3 from Cell Signalling.

Flow cytometry & analysis. Preparation of cells for flow cytometry, FlAsH labelling, and the cytometer configuration were as described previously (*26*). Cerulean and FlAsH fluorescence were collected using the Pacific blue (405 nm laser, 450/50 nm bandpass filter) and FITC (488 nm laser, 530/30 nm bandpass filter) channels, respectively.

Data were analyzed using FlowJo (TreeStar, Inc.) by gating for high expression (Cerulean fluorescence above 500 AFU) then for high or low FlAsH reactivity. The high FlAsH gate was defined as a diagonal line in a logarithmic FlAsH to Cerulean cytogram that was adjusted by translation so as to contain 80% cells expressing c-Src^{XTC}. The percent of high expressing cells with high FlAsH was calculated.

For drug screening, 6.6×10^4 COS-1 cells were transfected in solution with 0.32 μg c-Src^{XTC}-Cerulean DNA using 0.4 μL Lipofectamine 2000 and plated in 96-well tissue culture plates. The following day, cells were treated for 2 h with 5 μM drug or DMSO vehicle in HBSS. PP1 and PP2 were from Sigma and all other drug screen compounds were supplied by the Walter and Eliza Hall HTS group. FlAsH staining was performed as described previously (*3*). 100 μL cell suspension was analyzed using an LSRFortessa flow cytometer equipped with a high throughput sampler at 2.5 μL/sec. Three independent experiments were conducted with randomised compound locations. Concentration response curves were performed under the same conditions with 8 replicates. Half-maximal effective concentrations (EC_{50} values) were estimated by fitting to a four-parameter sigmoidal equation using Sigmaplot 12 (Systat).

Statistics. For the drug screen, percent high FlAsH values were normalised to plate means and standard deviations using the z-score method (*27*). Z-scores across replicates were compared to DMSO vehicle controls and hits were identified via a two-tailed t-test with respect to the DMSO control, with a cut-off of $p<0.05$.

Circular dichroism spectroscopy. Circular dichroism (CD) spectra of 0.2 mg/mL protein were measured in a 1 mm pathlength cuvette in 10 mM phosphate pH 7, 1 mM DTT at 20 °C using a model 410 SF CD spectrometer (Aviv) at 100 nm/min in continuous scanning mode with a 0.5 nm data-pitch. Final spectra were averages of 3 scans with buffer subtraction.

SH2 Binding assay. The phosphotyrosyl peptide corresponded to residues 321–331 of the hamster polyomavirus middle T antigen (NP_056731) phosphorylated at Tyr342 (pY) was synthesized commercially **(**GL Biochem) with FITC attached to the N-terminus via aminocaproic acid (Acp) (FITC-Acp-EPQpYEEIPIYL). Dilution

titrations were measured in 50 mM Tris pH 7.4, 150 mM NaCl, 12.5 mM imidazole, 1 mM TCEP using a Cary Eclipse fluorescence spectrophotometer with automated polarizers (Agilent Technologies). Equilibrium dissociation constant (K_d) values were calculated as described previously (*28*).

Information Available: Supplementary Tables 1 and 2 is made free of charge *via* the Internet at http://pubs.acs.org

ACKNOWLEDGEMENTS

The work was funded in part by grants to D.M.H. and T.D.M. from the Australian National Health and Medical Research Council and the Australian Research Council. D.M.H. was a Grimwade Fellow, supported by the Miegunyah Trust and currently an ARC Future Fellow. The Huang lab is supported by the Australian National Health and Medical Research Council (Program Grant 1016701; Independent Research Institutes Infrastructure Support Scheme grant 361646), the Leukemia and Lymphoma Society (SCOR grants) and a Victorian State Government Operational Infrastructure Support (OIS) Grant.

AUTHOR CONTRIBUTIONS

D.M.H. and T.D.M. conceived the sensor design, oversaw the project, its implementation and preparation of the manuscript. R.W. designed and performed experiments, interpreted data and co-wrote the manuscript. S.I. performed experiments, helped analyse data and assisted in drafting the manuscript. J.S. and Y.R. performed experiments, helped interpret data and contributed to the writing of

the manuscript. K.L. and D.C.S.H. contributed to the design of the drug screen and oversaw its implementation.

REFERENCES

1. Bermejo, C., Ewald, J. C., Lanquar, V., Jones, A. M. & Frommer, W. B. . (2011) *In vivo* biochemistry: quantifying ion and metabolite levels in individual cells or cultures of yeast, *Biochem. J. 438*, 1–10.
2. Griffin, B. A., Adams, S. R., and Tsien, R. Y. (1998) Specific Covalent Labeling of Recombinant Protein Molecules Inside Live Cells, *Science 281*, 269–272.
3. Ramdzan, Y. M., Nisbet, R. M., Miller, J., Finkbeiner, S., Hill, A. F., and Hatters, D. M. (2010) Conformation sensors that distinguish monomeric proteins from oligomers in live cells, *Chem. Biol. 17*, 371–379.
4. Luedtke, N. W., Dexter, R. J., Fried, D. B., and Schepartz, A. (2007) Surveying Polypeptide and Protein Domain Conformation and Association with FlAsH and ReAsH, *Nat. Chem. Biol. 3*, 779-784.
5. Ignatova, Z., and Gierasch, L. M. (2004) Monitoring Protein Stability and Aggregation *in vivo* by Real-time Fluorescent Labeling, *Proc. Natl. Acad. Sci. USA 101*, 523–528.
6. Playford, M. P., and Schaller, M. D. (2004) The interplay between Src and integrins in normal and tumor biology, *Oncogene 23*, 7928–7946.
7. Cowan-Jacob, S. W., Fendrich, G., Manley, P. W., Jahnke, W., Fabbro, D., Liebetanz, J., and Meyer, T. (2005) The Crystal Structure of a c-Src Complex in an Active Conformation Suggests Possible Steps in c-Src Activation, *Structure 13*, 861–871.
8. Xu, W., Harrison, S., and Eck, M. (1997) Three-dimensional structure of the tyrosine kinase c-Src, *Nature 385*, 595–602.
9. Wang, Y., Botvinick, E., Zhao, Y., Berns, M., Usami, S., Tsien, R., and Chien, S. (2005) Visualizing the mechanical activation of Src, *Nature 434*, 1040–1045.
10. Gulyani, A., Vitriol, E., Allen, R., Wu, J., Gremyachinskiy, D., Lewis, S., Dewar, B., Graves, L. M., Kay, B. K., and Kuhlman, B. (2011) A biosensor generated via high-throughput screening quantifies cell edge Src dynamics, *Nat. Chem. Biol. 7*, 437–444.
11. Karatan, E., Merguerian, M., Han, Z., Scholle, M. D., Koide, S., and Kay, B. K. (2004) Molecular Recognition Properties of FN3 Monobodies that Bind the Src SH3 Domain, *Chem. Biol. 11*, 835–844.
12. Adams, S. R., Campbell, R. E., Gross, L. A., Martin, B. R., Walkup, G. K., Yao, Y., Llopis, J., and Tsien, R. Y. (2002) New Biarsenical Ligands and Tetracysteine Motifs for Protein Labeling *In vitro* and *In vivo*: Synthesis and Biological Applications, *J. Am. Chem. Soc. 124*, 6063–6076.
13. Irtegun, S., Wood, R. J., Ormsby, A. R., Mulhern, T. D., and Hatters, D. M. (2013) Tyrosine 416 Is Phosphorylated in the Closed, Repressed Conformation of c-Src, *PLoS One 8*, e71035.
14. Sandilands, E., Cans, C., Fincham, V. J., Brunton, V. G., Mellor, H., Prendergast, G. C., Norman, J. C., Superti-Furga, G., and Frame, M. C. (2004)

RhoB and Actin Polymerization Coordinate Src Activation with Endosome-Mediated Delivery to the Membrane, *Dev. Cell 7*, 855–869.
15. Cooper, J. A., Gould, K. L., Cartwright, C. A., and Hunter, T. (1986) Tyr527 is phosphorylated in pp60c-src: implications for regulation, *Science 231*, 1431–1434.
16. Yi, L., and Gray, N. S. (2006) Rational design of inhibitors that bind to inactive kinase conformations, *Nat. Chem. Biol. 2*, 358-364.
17. Levinson, N. M., and Boxer, S. G. (2013) A conserved water-mediated hydrogen bond network defines bosutinib's kinase selectivity, *Nat. Chem. Biol*. *10*, 127–132
18. Brave, S. R., Odedra, R., James, N. H., Smith, N. R., Marshall, G. B., Acheson, K. L., Baker, D., Howard, Z., Jackson, L., and Ratcliffe, K. (2011) Vandetanib inhibits both VEGFR-2 and EGFR signalling at clinically relevant drug levels in preclinical models of human cancer, *Int. J. Oncol. 39*, 271–278.
19. Jia, H.-Y., Wu, J.-X., Zhu, X.-F., Chen, J.-M., Yang, S.-P., Yan, H.-J., Tan, L., Zeng, Y.-X., and Huang, W. (2009) ZD6474 inhibits Src kinase leading to apoptosis of imatinib-resistant K562 cells, *Leuk. Res. 33*, 1512–1519.
20. Harrington, E. A., Bebbington, D., Moore, J., Rasmussen, R. K., Ajose-Adeogun, A. O., Nakayama, T., Graham, J. A., Demur, C., Hercend, T., Diu-Hercend, A., Su, M., Golec, J. M., and Miller, K. M. (2004) VX-680, a potent and selective small-molecule inhibitor of the Aurora kinases, suppresses tumor growth in vivo, *Nat. Med. 10*, 262–267.
21. Wang, S., Midgley, C. A., Scaërou, F., Grabarek, J. B., Griffiths, G., Jackson, W., Kontopidis, G., McClue, S. J., McInnes, C., and Meades, C. (2010) Discovery of N-phenyl-4-(thiazol-5-yl) pyrimidin-2-amine aurora kinase inhibitors, *J. Med. Chem. 53*, 4367–4378.
22. Bain, J., Plater, L., Elliott, M., Shpiro, N., Hastie, C., Mclauchlan, H., Klevernic, I., Arthur, J., Alessi, D., and Cohen, P. (2007) The selectivity of protein kinase inhibitors: a further update, *Biochem. J 408*, 297–315.
23. Karni, R., Mizrachi, S., Reiss-Sklan, E., Gazit, A., Livnah, O., and Levitzki, A. (2003) The pp60(c-Src) inhibitor PP1 is non-competitive against ATP, *FEBS Lett. 537*, 47–52.
24. Han, X., Yamanouchi, G., Mori, T., Kang, J.-H., Niidome, T., and Katayama, Y. (2009) Monitoring protein kinase activity in cell lysates using a high-density peptide microarray, *J. Biomol. Screen. 14*, 256–262.
25. Olshina, M. A., Angley, L. M., Ramdzan, Y. M., Tang, J., Bailey, M. F., Hill, A. F., and Hatters, D. M. (2010) Tracking mutant huntingtin aggregation kinetics in cells reveals three major populations that include an invariant oligomer pool, *J. Biol. Chem. 285*, 21807–21816.
26. Ramdzan, Y. M., Polling, S., Chia, C. P., Ng, I. H., Ormsby, A. R., Croft, N. P., Purcell, A. W., Bogoyevitch, M. A., Ng, D. C., Gleeson, P. A., and Hatters, D. M. (2012) Tracking protein aggregation and mislocalization in cells with flow cytometry, *Nat. Methods 9*, 467–470.
27. Brideau, C., Gunter, B., Pikounis, B., and Liaw, A. (2003) Improved Statistical Methods for Hit Selection in High-Throughput Screening, *J. Biomol. Screen. 8*, 634–647.
28. Mills, R. D., Trewhella, J., Qiu, T. W., Welte, T., Ryan, T. M., Hanley, T., Knott, R. B., Lithgow, T., and Mulhern, T. D. (2009) Domain organization of the monomeric form of the Tom70 mitochondrial import receptor, *J. Mol. Biol. 388*, 1043–1058.

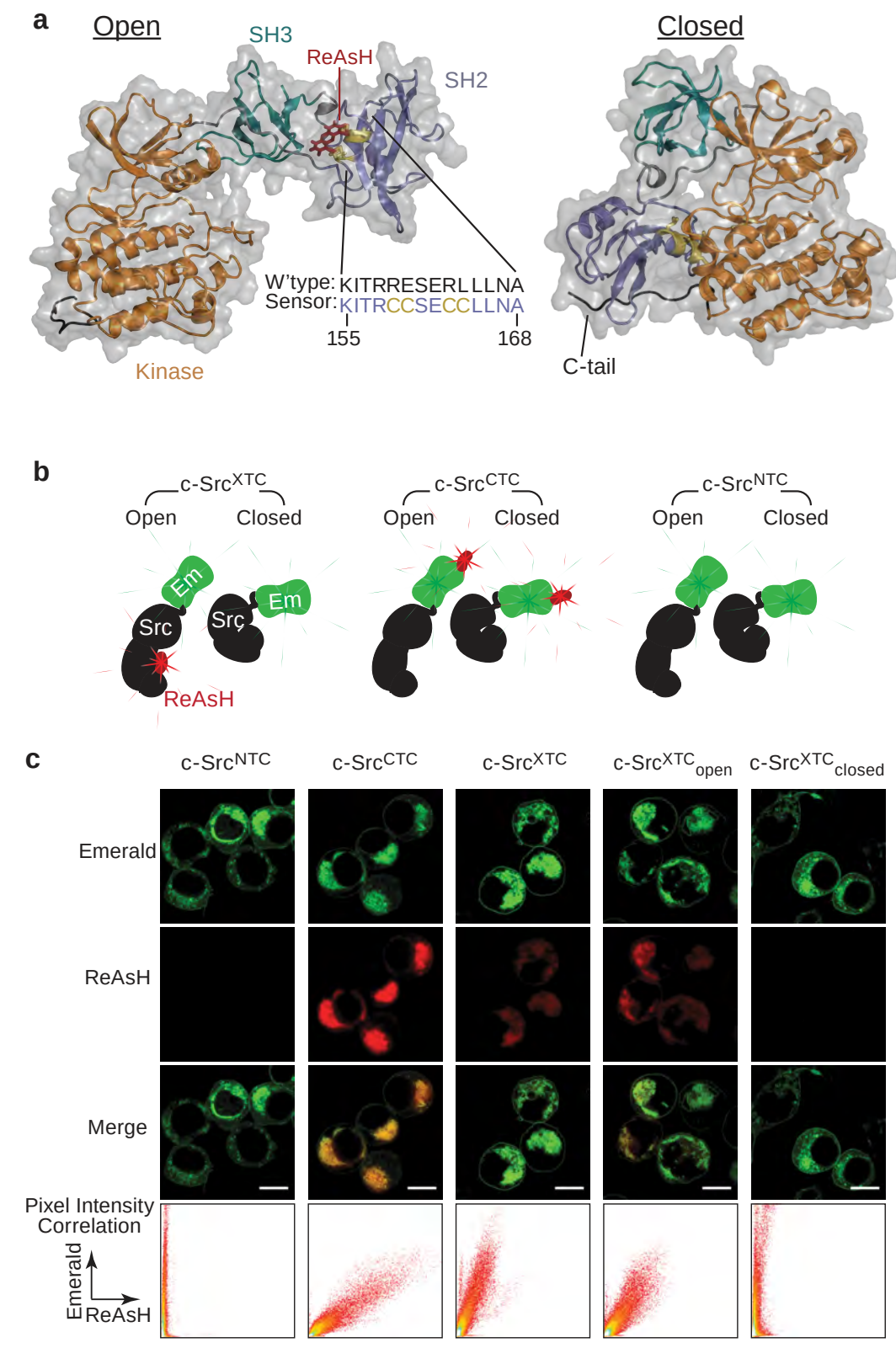
a
Open
SH3
ReAsH
SH2
Closed
W'type: KITRRESERLLLNA
Sensor: KITRCCSECCLLNA
155
168
Kinase
C-tail
b
c-SrcXTC
Open
Closed
c-SrcCTC
Open
Closed
c-SrcNTC
Open
Closed
Em
Em
Src
Src
ReAsH
c
c-SrcNTC
c-SrcCTC
c-SrcXTC
c-SrcXTC open
c-SrcXTC closed
Emerald
ReAsH
Merge
Pixel Intensity Correlation
Emerald
ReAsH

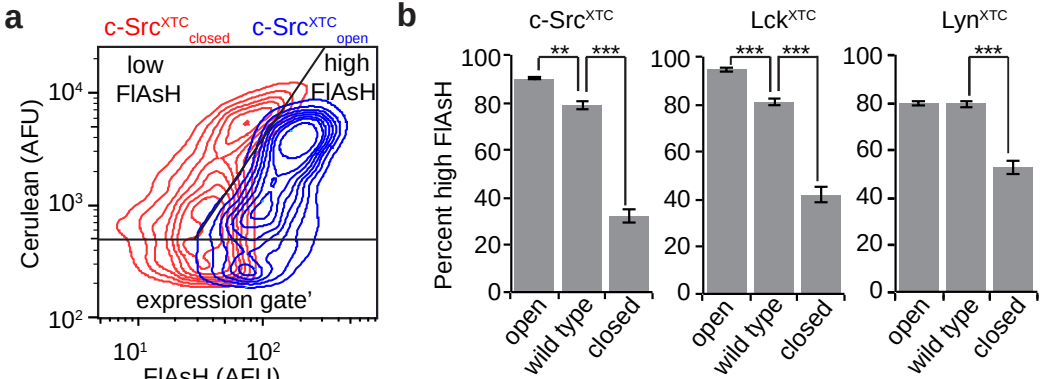
a
c-Src^XTC closed
c-Src^XTC open
low FlAsH
high FlAsH
expression gate'
Cerulean (AFU)
FlAsH (AFU)
b
c-Src^XTC
Lck^XTC
Lyn^XTC
Percent high FlAsH
**
***
open
wild type
closed

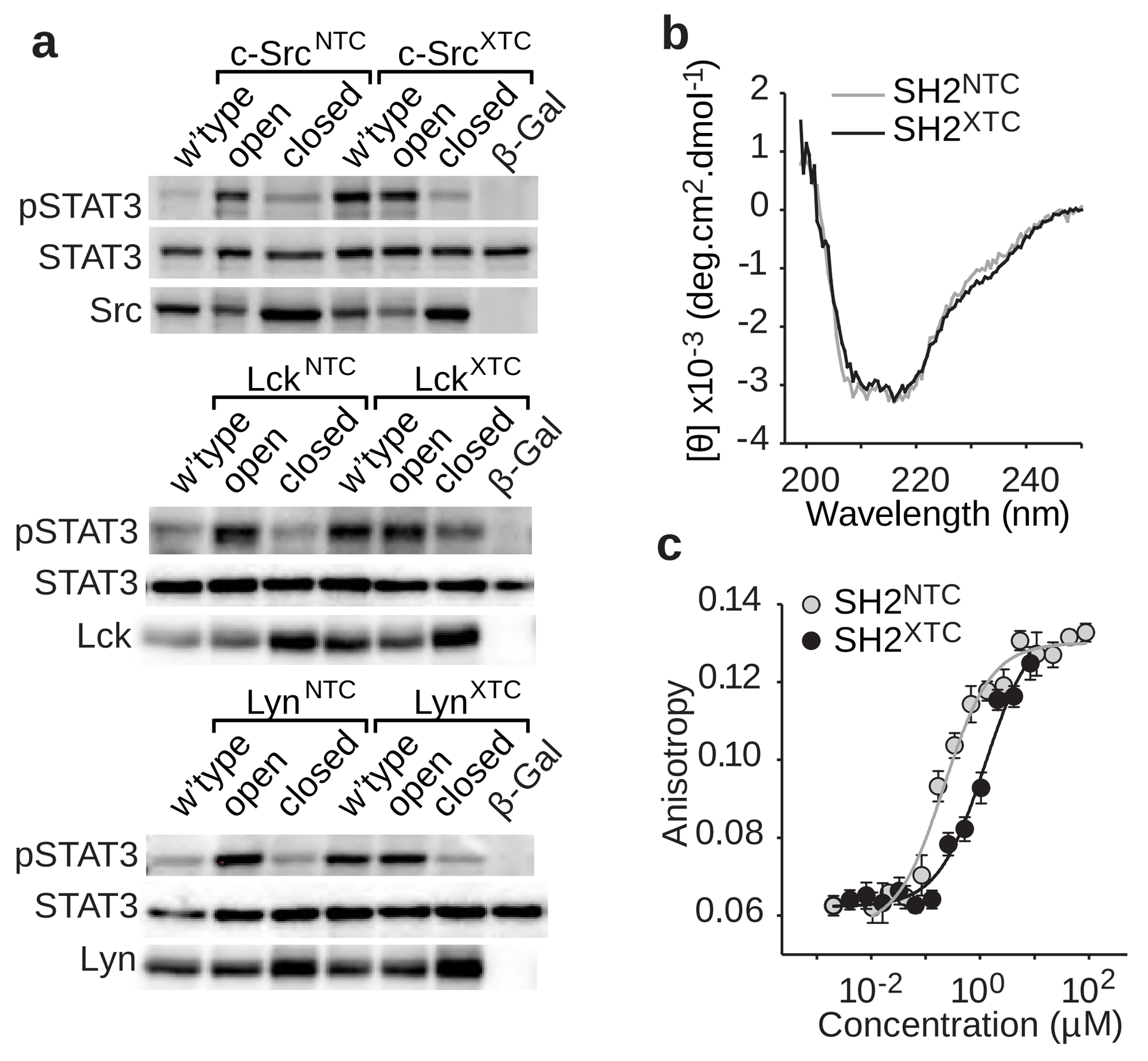
a
c-Src NTC
c-Src XTC
w'type
open
closed
w'type
open
closed
β-Gal
pSTAT3
STAT3
Src
Lck NTC
Lck XTC
w'type
open
closed
w'type
open
closed
β-Gal
pSTAT3
STAT3
Lck
Lyn NTC
Lyn XTC
w'type
open
closed
w'type
open
closed
β-Gal
pSTAT3
STAT3
Lyn
b
SH2NTC
SH2XTC
[θ] x10-3 (deg.cm2.dmol-1)
2
1
0
-1
-2
-3
-4
200
220
240
Wavelength (nm)
c
SH2NTC
SH2XTC
Anisotropy
0.14
0.12
0.10
0.08
0.06
10-2
100
102
Concentration (μM)

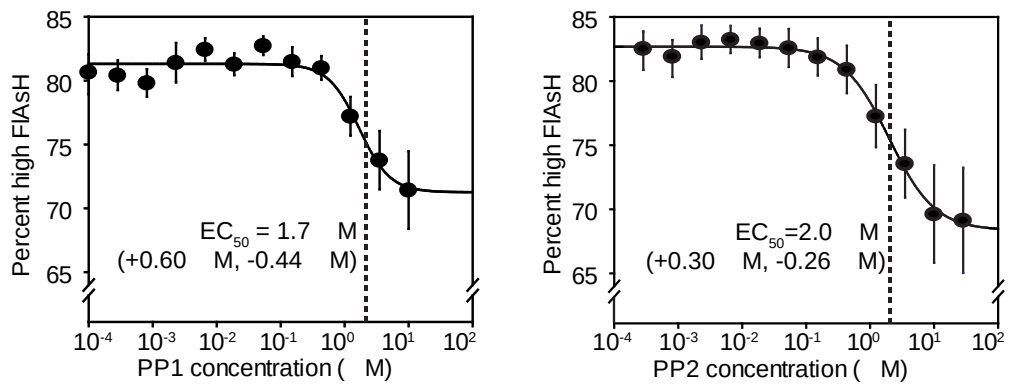
85
80
75
70
65
Percent high FlAsH
EC50 = 1.7 M
(+0.60 M, -0.44 M)
10-4 10-3 10-2 10-1 100 101 102
PP1 concentration (M)
85
80
75
70
65
Percent high FlAsH
EC50=2.0 M
(+0.30 M, -0.26 M)
10-4 10-3 10-2 10-1 100 101 102
PP2 concentration (M)

A biosensor of Src family kinase conformation by exposable tetracysteine useful for cell-based screening.

Sevgi Irtegun[1,2], Rebecca Wood[1,2], Kurt Lackovic[3, 4], Jörg Schweiggert[1], Yasmin M. Ramdzan[1], David C.S. Huang[3,4], Terrence D. Mulhern[1*] & Danny M. Hatters[1*]

[1]Department of Biochemistry and Molecular Biology; and Bio21 Molecular Science and Biotechnology Institute, University of Melbourne, VIC 3010.

[2]Equally contributed to the work.

[3]Walter and Eliza Hall Institute of Medical Research, VIC 3010

[4]Department of Medical Biology, University of Melbourne, VIC 3010

*Correspondence should be addressed to D.M.H. (dhatters@unimelb.edu.au) or T.D.M. (tmulhern@unimelb.edu.au) . Ph: +61 38344 2530.

SUPPLEMENTARY TABLES

Supplementary Table 1: Amino acid sequences of the basic sensor constructs.

c-Src^{xtc}-Cerulean • Linker in gray • Cerulean in cyan • TC in orange	MGSNKSKPKDASQRRRSLEPAENVHGAGGGAFPASQTPSKPASADGHRGPSAAF APAAAEPKLFGGFNSSDTVTSPQRAGPLAGGVTTFVALYDYESRTETDLSFKKGE RLQIVNNTEGDWWLAHSLSTGQTGYIPSNYVAPSDSIQAEEWYFGKITRCCSECC LLNAENPRGTFLVRESETTKGAYCLSVSDFDNAKGLNVKHYKIRKLDSGGFYITS RTQFNSLQQLVAYYSKHADGLCHRLTTVCPTSKPQTQGLAKDAWEIPRESLRLEV KLGQGCFGEVWMGTWNGTTRVAIKTLKPGTMSPEAFLQEAQVMKKLRHEKLVQ LYAVVSEEPIYIVTEYMSKGSLLDFLKGETGKYLRLPQLVDMAAQIASGMAYVER MNYVHRDLRAANILVGENLVCKVADFGLARLIEDNEYTARQGAKFPIKWTAPEA ALYGRFTIKSDVWSFGILLTELTTKGRVPYPGMVNREVLDQVERGYRMPCPPECP ESLHDLMCQCWRKEPEERPTFEYLQAFLEDYFTSTEPQYQPGENLGSGSDPPVAT GSLVSKGEELFTGVVPILVELDGDVNGHKFSVSGEGEGDATYGKLTLKFICTTGK LPVPWPTLVTTLTWGVQCFARYPDHMKQHDFFKSAMPEGYVQERTIFFKDDGNY KTRAEVKFEGDTLVNRIELKGIDFKEDGNILGHKLEYNAISDNVYITADKQKNGIK ANFKIRHNIEDGSVQLADHYQQNTPIGDGPVLLPDNHYLSTQSKLSKDPNEKRDH MVLLEFVTAAGITLGMDELYK
c-Src^{ctc}-Emerald • Linker in gray • Emerald in green • TC in orange	MGSNKSKPKDASQRRRSLEPAENVHGAGGGAFPASQTPSKPASADGHRGPSAAF APAAAEPKLFGGFNSSDTVTSPQRAGPLAGGVTTFVALYDYESRTETDLSFKKGE RLQIVNNTEGDWWLAHSLSTGQTGYIPSNYVAPSDSIQAEEWYFGKITRRESERLL LNAENPRGTFLVRESETTKGAYCLSVSDFDNAKGLNVKHYKIRKLDSGGFYITSR TQFNSLQQLVAYYSKHADGLCHRLTTVCPTSKPQTQGLAKDAWEIPRESLRLEVK LGQGCFGEVWMGTWNGTTRVAIKTLKPGTMSPEAFLQEAQVMKKLRHEKLVQL YAVVSEEPIYIVTEYMSKGSLLDFLKGETGKYLRLPQLVDMAAQIASGMAYVER MNYVHRDLRAANILVGENLVCKVADFGLARLIEDNEYTARQGAKFPIKWTAPEA ALYGRFTIKSDVWSFGILLTELTTKGRVPYPGMVNREVLDQVERGYRMPCPPECP ESLHDLMCQCWRKEPEERPTFEYLQAFLEDYFTSTEPQYQPGENLGSGSDPPVAT GSLVSKGEELFTGVVPILVELDGDVNGHKFSVSGEGEGDATYGKLTLKFICTTGK LPVPWPTLVTTLTYGVQCFARYPDHMKQHDFFKSAMPEGYVQERTIFFKDDGNY KTRAEVKFEGDTLVNRIELKGIDFKEDGNILGHKLEYNYNSHKVYITADKQKNGI KVNFKTRHNIEDGSVQLADHYQQNTPIGDGPVLLPDNHYLSTQSKLSKDPNEKRD HMVLLEFVTAAGITLGMDELYKEAAAREACCPGCCARA
Lyn^{xtc}-Cerulean • Linker in gray • Cerulean in cyan • TC in orange	MGCIKSKGKDSLSDDGVDLKTQPVRNTERTIYVRDPTSNKQQRPVPESQLLPGQR FQTKDPEEQGDIVVALYPYDGIHPDDLSFKKGEKMKVLEEHGEWWKAKSLLTKK EGFIPSNYVAKLNTLETEEWFFKDITRCCAECCLLAPGNSAGAFLIRESETLKGSFS LSVRDFDPVHGDVIKHYKIRSLDNGGYYISPRITFPCISDMIKHYQKQADGLCRRLE KACISPKPQKPWDKDAWEIPRESIKLVKRLGAGQFGEVWMGYYNNSTKVAVKTL KPGTMSVQAFLEEANLMKTLQHDKLVRLYAVVTREEPIYIITEYMAKGSLLDFLK SDEGGKVLLPKLIDFSAQIAEGMAYIERKNYIHRDLRAANVLVSESLMCKIADFGL ARVIEDNEYTAREGAKFPIKWTAPEAINFGCFTIKSDVWSFGILLYEIVTYGKIPYP GRTNADVMTALSQGYRMPRVENCPDELYDIMKMCWKEKAEERPTFDYLQSVLD DFYTATEGQYQQQPGSGSGSDPPVATGSLVSKGEELFTGVVPILVELDGDVNGHK FSVSGEGEGDATYGKLTLKFICTTGKLPVPWPTLVTTLTWGVQCFARYPDHMKQ HDFFKSAMPEGYVQERTIFFKDDGNYKTRAEVKFEGDTLVNRIELKGIDFKEDGNI LGHKLEYNAISDNVYITADKQKNGIKANFKIRHNIEDGSVQLADHYQQNTPIGDGP VLLPDNHYLSTQSKLSKDPNEKRDHMVLLEFVTAAGITLGMDELYK
Lck^{xtc}-Cerulean • Linker in gray	MGCGCSSHPEDDWMENIDVCENCHYPIVPLDGKGTLLIRNGSEVRDPLVTYEGSN PPASPLQDNLVIALHSYEPSHDGDLGFEKGEQLRILEQSGEWWKAQSLTTGQEGFI PFNFVAKANSLEPEPWFFKNLSRCCAECCLLAPGNTHGSFLIRESESTAGSFSLSVR DFDQNQGEVVKHYKIRNLDNGGFYISPRITFPGLHELVRHYTNASDGLCTRLSRPC QTQKPQKPWWEDEWEVPRETLKLVERLGAGQFGEVWMGYYNGHTKVAVKSLK QGSMSPDAFLAEANLMKQLQHQRLVRLYAVVTQEPIYIITEYMENGSLVDFLKTP

● Cerulean in cyan TC in orange	SGIKLTINKLLDMAAQIAEGMAFIEERNYIHRDLRAANILVSDTLSCKIADFGLARL IEDNEYTAREGAKFPIKWTAPEAINYGTFTIKSDVWSFGILLTEIVTHGRIPYPGMT NPEVIQNLERGYRMVRPDNCPEELYQLMRLCWKERPEDRPTFDYLRSVLEDFFTA TEGQYQPQPAGSGSGSDPPVATGSLVSKGEELFTGVVPILVELDGDVNGHKFSVS GEGEGDATYGKLTLKFICTTGKLPVPWPTLVTTLTWGVQCFARYPDHMKQHDFF KSAMPEGYVQERTIFFKDDGNYKTRAEVKFEGDTLVNRIELKGIDFKEDGNILGH KLEYNAISDNVYITADKQKNGIKANFKIRHNIEDGSVQLADHYQQNTPIGDGPVLL PDNHYLSTQSKLSKDPNEKRDHMVLLEFVTAAGITLGMDELYK

Supplementary Table 2: results of the kinase inhibitor screen highlighting hits for c-Src closure

Drug name	Z-scores for replicates			Mean	Standard Deviation	p value
	1	2	3			
Vandetanib	-1.014	-1.135	-1.031	-1.060	0.066	0.002
CI-1040	0.605	0.545	0.500	0.550	0.053	0.002
VX745	0.777	0.993	1.082	0.951	0.157	0.007
CP-724714	1.757	1.513	1.237	1.502	0.260	0.009
PP2	-1.056	-1.485	-1.186	-1.242	0.220	0.012
CYC-116	-3.074	-2.151	-2.397	-2.541	0.478	0.013
Canertinib	2.551	1.685	2.378	2.205	0.458	0.013
Sorafenib	0.890	0.515	0.765	0.723	0.191	0.017
Regorafenib	0.747	0.909	0.500	0.719	0.206	0.020
Tozasertib	-0.819	-0.667	-1.029	-0.838	0.182	0.020
AC220	0.608	1.040	1.134	0.927	0.281	0.023
SMI-4a	1.723	1.253	2.345	1.774	0.548	0.027
SB203580	1.216	0.946	0.593	0.918	0.313	0.029
Barasertib	0.645	0.978	0.490	0.704	0.250	0.030
Ridaforolimus	2.317	1.277	1.329	1.641	0.586	0.035
PP1	-1.744	-2.057	-1.049	-1.616	0.516	0.037
Dianilinopyrimidine 0	-0.968	-2.011	-1.958	-1.646	0.588	0.046
Sunitinib	0.176	0.245	0.559	0.327	0.204	0.066
GSK2126458	-0.507	-0.638	-1.082	-0.743	0.302	0.069
E7080	0.605	0.121	0.441	0.389	0.246	0.072
PD173955-Analogue 1	0.616	1.141	0.350	0.702	0.403	0.073
Pazopanib	-0.946	-1.277	-0.464	-0.895	0.409	0.080
KU-60019	0.304	1.017	0.464	0.595	0.374	0.082
SU-6668	0.101	0.638	0.670	0.470	0.320	0.088
GSK-25	0.534	1.909	0.882	1.108	0.715	0.098
AG-490	0.101	0.875	0.851	0.609	0.440	0.105
Vatalanib	0.203	1.440	1.189	0.944	0.654	0.108
Masatinib	1.554	0.598	0.420	0.857	0.610	0.111
Saracatinib	-1.284	-2.364	-0.696	-1.448	0.846	0.112
Enzastaurin	0.792	0.190	1.329	0.770	0.570	0.115
JNJ38877605	0.747	0.152	1.206	0.702	0.529	0.117
SD169	0.304	0.496	1.392	0.731	0.580	0.128
Ruxolitinib	0.463	0.182	1.147	0.597	0.496	0.132
Danusertib	-1.486	-0.449	-2.345	-1.427	0.949	0.139
Axitinib	0.980	0.426	0.077	0.494	0.455	0.148
JNJ7706621	0.147	0.625	0.070	0.281	0.301	0.153
AMG-Tie2-1	-3.203	-1.152	-0.706	-1.687	1.332	0.177
Imatinib mesylate	0.439	0.591	-0.103	0.309	0.365	0.184

BMS 794833	-0.117	1.304	0.839	0.675	0.725	0.201
Tofacitinib	-0.264	-0.652	-1.678	-0.865	0.731	0.216
Foretinib	-1.701	0.054	-1.888	-1.178	1.072	0.227
AEE788	-0.405	-1.584	-0.335	-0.775	0.702	0.243
Dasatinib	-0.178	-2.152	-0.824	-1.051	1.006	0.247
Motesanib	0.890	0.939	-0.265	0.521	0.681	0.249
BX795	0.961	1.455	-0.529	0.629	1.033	0.340
PD153035	-1.173	-0.652	0.140	-0.562	0.661	0.360
Selumetinib	-2.111	0.190	-0.629	-0.850	1.167	0.387
PLX4720	-0.203	-0.071	-1.057	-0.443	0.535	0.396
Pelitinib	-1.032	0.030	-0.324	-0.442	0.541	0.402
PF-2341066	0.036	-0.212	0.971	0.265	0.624	0.405
Nilotinib	1.655	0.024	-0.206	0.491	1.015	0.412
RAF265	1.085	-0.217	0.000	0.289	0.698	0.424
PIK-294	-0.440	0.408	0.420	0.129	0.493	0.486
NVP-TAE684	0.088	0.000	-2.853	-0.922	1.673	0.490
AT-7519	-0.320	-2.818	0.382	-0.919	1.682	0.494
BI-2536(R-)	-0.101	-0.213	0.361	0.016	0.304	0.544
Cediranib	-0.557	0.054	-0.210	-0.238	0.307	0.552
ENMD-2076	-0.264	0.082	-0.490	-0.224	0.288	0.570
R406	-1.993	-0.364	0.618	-0.580	1.319	0.602
Erlotinib	-1.182	0.189	-0.077	-0.357	0.727	0.619
Bosutinib	-0.821	-0.978	0.629	-0.390	0.886	0.641
Seliciclib	0.107	-0.121	-0.206	-0.073	0.162	0.721
Tandutinib	-0.528	-0.598	0.420	-0.235	0.568	0.743
SB202190	-0.176	-0.408	0.559	-0.008	0.505	0.756
Linifanib	0.783	0.909	-3.206	-0.505	2.340	0.799
Afatinib	-0.391	0.273	-0.412	-0.177	0.389	0.800
Quercetin	-0.890	-0.030	1.000	0.027	0.946	0.823
SNS-032	-0.642	0.284	0.103	-0.085	0.491	0.933
PF-562271	-0.178	0.636	-0.706	-0.082	0.676	0.947
SU-5402	-0.285	-0.455	0.353	-0.129	0.426	0.952
CHIR-99021	0.147	1.630	-2.028	-0.084	1.840	0.981
Gefitinib	0.712	-1.758	0.706	-0.113	1.424	0.999

Author/s:
Irtegun, S; Wood, R; Lackovic, K; Schweiggert, J; Ramdzan, YM; Huang, DCS; Mulhern, TD; Hatters, DM

Title:
A Biosensor of Src Family Kinase Conformation by Exposable Tetracysteine Useful for Cell-Based Screening

Date:
2014-07-01

Citation:
Irtegun, S., Wood, R., Lackovic, K., Schweiggert, J., Ramdzan, Y. M., Huang, D. C. S., Mulhern, T. D. & Hatters, D. M. (2014). A Biosensor of Src Family Kinase Conformation by Exposable Tetracysteine Useful for Cell-Based Screening. ACS CHEMICAL BIOLOGY, 9 (7), pp.1426-1431. https://doi.org/10.1021/cb500242q.